2013 IEEE 10th International Symposium on Biomedical Imaging:
From Nano to Macro
San Francisco, CA, USA, April 7-11, 2013

PROPAGATION OF THE MRI PROSTATE DELINEATION TO THE PLANNING CT: A NEW MATCHING CONTOUR FRAMEWORK

Frédéric Commandeur[1,2], *Oscar Acosta*[1,2], *Antoine Simon*[1,2], *Romain Mathieu*[3], *Pascal Haigron*[1,2] *and Renaud de Crevoisier*[1,2,4]

[1]INSERM, U1099, Rennes, F-35000, France;
[2]Université de Rennes 1, LTSI, Rennes, F-35000, France;
[3]Department of Urology, CHU Pontchaillou, Rennes, F-35000, France;
[4]Department of Radiotherapy, Centre Eugène Marquis, Rennes, F-35000, France

ABSTRACT

Although accurate delineations of the prostate on computed tomography (CT) images are required for the planning in prostate cancer radiotherapy, these images do not provide the reliable soft tissue contrast. On the contrary, magnetic resonance (MR) images offer the possibility to better delineate both the tumor and healthy prostate tissues. Because CT is still used during the planning, MRI-CT image registration is an essential step to improve the targeting. In this paper, we propose a new framework to propagate the MRI prostate delineation to the CT-scan based on a robust contour matching approach. Prostate boundaries in CT are characterized with several multi-scale features and detected with a support vector machine (SVM) classifier. A new cost function for aligning the MRI delineation to the detected contours was developed. We evaluated the proposed approach on 11 manually aligned and delineated MR and CT images. The method outperformed the widely used mutual information (MI) and demonstrated the drawbacks of this metric for this application.

Index Terms— MRI, CT, Registration, Prostate, Radiotherapy

1. INTRODUCTION

Modern strategies in prostate cancer radiotherapy such as intensity modulated radiotherapy (IMRT) allow to achieve high precision in delivering the dose, provided an accurate target definition. In nowadays planning, CT is still used to perform this task as dose computation relies on CT electron density information. However, CT offers a poor soft tissue contrast and segmenting prostate is prone to errors, especially in the apical and basis regions. These uncertainties lead to large intra- and inter-observer variability and may impact the treatment planning [1] and dosimetry [2].

On the contrary, because MRI provides high definition of tumor and healthy tissues, accurate MRI-CT image registration becomes an essential step to improve target delineation. Because the prostate does not present large deformations [6] and prostate shapes may be almost identically in both MR and CT images, rigid transformation is allowed.

An accurate prostate alignment can be achieved after rigid registration using gold markers as fiducials [3, 4] which also may be used for validation. However, this is an invasive procedure, which is less clinically performed. In addition, in some cases these markers are barely noticeable in MRI.

Alternatively, mutual information (MI) has been used as a cost function in automatic or semi-automatic methods to register prostate MR and CT images [5]. However, for prostate alignment, MI suffers from several drawbacks. Firstly, the results may considerably differ, depending on the region of interest (ROI) where the intensity information lies. Particularly, the performances may be strongly ROI-dependent on the pelvic region because of the neighboring structures, such as the rectum, the bladder and the femoral heads, that may hamper the reliability of the similarity measure. Manually defining localized regions to attenuate this dependency requires an intermediate cumbersome stage introducing observer variability.

As opposed to intensity-based registration, salient points and contours, characterized by multi-scale features, may introduce additional constraints to drive the registration. Algorithms based on Chamfer distance [7, 8], are very common to align contours but require all contours to be defined. Automatic or semi-automatic features and contours extraction in both images have been used as a previous step for registration [9, 10, 11].

In this paper we propose a new framework, depicted in figure 1, to propagate the MRI prostate manual delineation to the CT. It is decomposed in two steps: (i) an automatic prostate contours detection in CT, based on a support vector machine (SVM) classification with extracted features, and (ii) a rigid registration using the collinearity of the gradient vectors as a similarity measure.

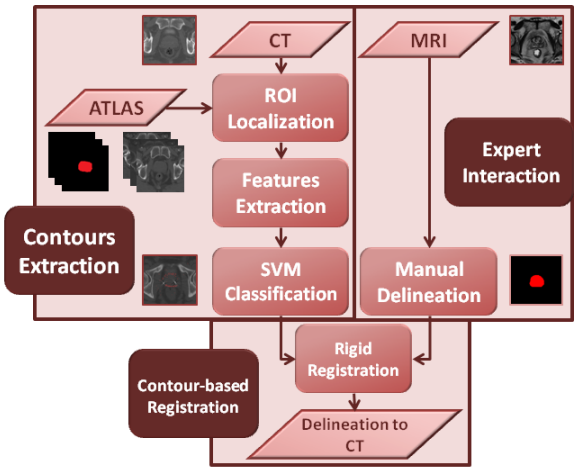

Fig. 1. Framework of the proposed method.

2. METHOD

2.1. Prostate Contour Extraction in the CT image

We propose an approach using an SVM classification based on features to detect prostate contour in CT. These features were computed at each voxel to form an anatomical signature. Moreover, as it has been used in [12], a patch-based method was considered by including the computed features over the neighborhood of each voxel into its own signature.

2.1.1. Features

Features providing informations on frequency and orientations were extracted in axial slices and used to distinguish voxels of the prostate boundaries from others, such as

- Gabor wavelets with different scales and orientations

$$\mathcal{G}(x,y) = exp\left(\frac{2i\pi x_\theta}{\lambda}\right) exp\left(-\frac{x_\theta^2+\gamma^2 y_\theta^2}{2\sigma^2}\right) \quad (1)$$

  with $x_\theta = xcos\theta + ysin\theta$ and $y_\theta = -xsin\theta + ycos\theta$, where θ denotes the orientation, γ the spatial ratio between the two dimensions, λ the wavelength of the sine and σ the scale factor of the Gaussian envelope.

- Haar-like features [13].
- Gradient vectors $\nabla_i = \left[\frac{\partial I_i}{\partial x}, \frac{\partial I_i}{\partial y}\right]$.

2.1.2. Feature Selection

A two-sample t-test was performed between feautures from contour voxels and others, in order to select only significant features improving prostate contours characterization. Anatomical signatures were composed with features which the associated p-value, resulting from the t-test, was inferior to 0.005.

2.1.3. SVM Classification

Let b_i be the anatomical signature of the voxel x_i, and y_i its corresponding label, $y_i = 1$ if voxel x_i belongs to the prostate contour, $y_i = -1$ otherwise. The training set $\{(b_1, y_1), ..., (b_N, y_N)\} \subset \mathbb{R}^m \times \{-1, 1\}$ is composed by N samples with known label and $m \times L \times L$ extracted features where m denotes the number of features and $L \times L$ defines the area of the neighborhood. We assumed our set to be linearly non-separable, and a Gaussian radial basis function was used as the kernel function $\Phi(b)$ to apply the kernel trick algorithm. The hyperplane that best separates both classes is $h(b) = w^T\Phi(b) + w_0$ where w and w_0 are respectively the vector containing weights associated to the selected features and w_0 the intercept, resulting from the training. The interest of the following proposed similarity is to match contours, even when there is an important lack of information. Thus, in order to be very selective and to detect almost only voxels which belong to the prostate contours, a receiver operating characteristic (ROC) analysis was performed and the value of the intercept was fixed to obtain a certain false positive (FP) rate, and an associated true positive (TP) rate or sensitivity, with the TP case defined as a well classified contour voxel and the FP case as a misclassified non-contour voxel.

2.2. Similarity Measure Based On Contours

Once prostate contours were partially extracted on CT, the idea was to fit them with the contours obtained from the expert manual delineation on MRI. To do this, we proposed to maximize the collinearity between the gradient vectors of these contours. Let ∇_{CT} and ∇_{MRI} be respectively the gradient fields of the extracted contours on CT and the manual delineation on MRI. The perfect alignment between these two gradient fields can be obtained while maximizing the collinearity over the common region denoted by Ω. To make the optimization process converge to the global maximum, the previous measure was smoothed by convolving gradient fields with a centred Gaussian kernel G_σ of variance σ^2. Thus, if $\nabla_{CT_\sigma} = G_\sigma * \nabla_{CT}$ and $\nabla_{MRI_\sigma} = G_\sigma * \nabla_{MRI}$ correspond respectively to the smoothed gradient fields of CT edges and MRI delineation, the gradient colinearity (GC) is defined as

$$GC(\nabla_{CT_\sigma}, \nabla_{MRI_\sigma}) = \frac{1}{|\Omega|}\sum_{x\in\Omega} \frac{\nabla_{CT_\sigma}(x)}{||\nabla_{CT_\sigma}(x)||} \cdot \frac{\nabla_{MRI_\sigma}(x)}{||\nabla_{MRI_\sigma}(x)||} \quad (2)$$

2.3. Coarse initialization to speed up the process

Computing the proposed features over the all image might be time consuming. To speed up the features extraction, an atlas-based coarse initialization is achieved to determine the prostate region of interest (ROI). Atlas-based methods have been largely used in the medical image domain for prostate segmentation in CT images [14], multi-modality registration [15] or at the basis of statistical analysis. To initialize the prostate position, the CT atlas used in [14] was registered on the CT query patient and the associated probability map was propagated. The center of mass of the prostate probability map was used to initialize the position of the MRI delineation and features used for contours detection were extracted from voxels with non zero associated probability.

3. RESULTS

3.1. Experiments

An atlas was created by rigidly registering 70 CT-scan of prostate cancer patients treated with external radiotherapy and propagating associated manual delineation in a common referential, to both train the SVM classifier and initialize the target ROI. Prostate registration were carried out on 11 different patients, who underwent a T2-MRI acquisition and a planning CT-scan. For each of these 11 patients, both images were manually co-registered by an expert to define the reference alignment. The same expert performed prostate manual delineation on MRI in the CT-scan referential. Later, an other expert validated alignments and delineations. A restricted ROI was manually defined on the CT images by delimiting a margin of 1 cm around the manual delineations boundaries. Rigid registrations were achieved using the proposed framework and two MI-based registrations: one using the ROI defined by the atlas and one using a more restricted ROI around the prostate. For each of the 11 patients, registration accuracy was assessed by evaluating the Dice coefficient defined as $Dice = 2|A \cap B|/|A + B|$, where A and B denote the two structures to be compared and $|.|$ the cardinal number, and the Hausdorff distance [16] between original and registered delineations.

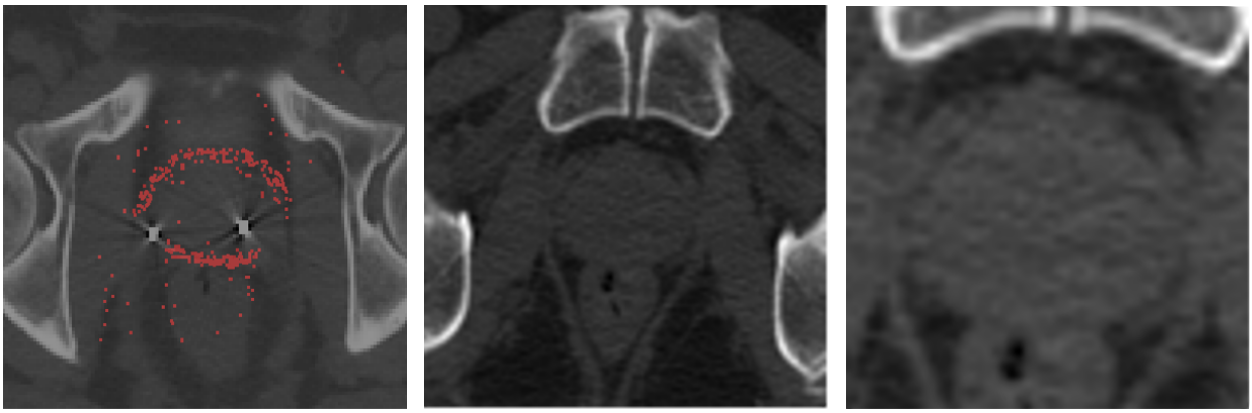

(a) Prostate contours partially extracted on a CT image.

(b) ROI used by the proposed method and the classic MI.

(c) ROI used by the restricted MI.

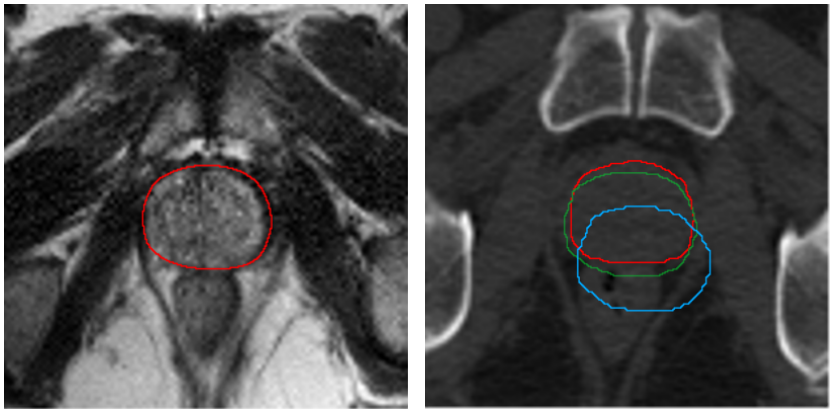

(d) MRI corresponding to the CT in figures 2(b) and 2(c), with the manual delineation.

(e) Propagation results of the three methods.

Fig. 2. Figure 2(a) presents an example of the results obtained from the contours extraction method where red voxels correspond to contour classified voxels. Examples of ROIs used are shown in figure 2(b) for the proposed similarity measure and the MI, and in figure 2(c) for the restricted MI.Corresponding MRI is presented in figure 2(d) with the associated manual delineation. Propagation of the delineation are shown in figure 2(e): the proposed method in red, the restricted MI in green and the classic MI in blue.

3.2. Contour Extraction

The SVM classification associated with the ROC analysis according to the intercept w_0 allowed to be selective on the contours detection. The t-test allowed to reduce the initial number of features from 2000 to 100. Optimal features selected for prostate contours identification were features describing high frequencies, small scales and diagonal orientations. The ROC curve is plotted in figure 3. An FP rate of 10% was chosen, leading to an associated TP rate of 57%. An example of the extracted contours is shown in figure 2(a) where red voxels correspond to contour classified voxels.

3.3. Registration

The table 1 presents mean scores obtained for the three mentioned methods and figures 4(a) and 4(c) described respectively Dice scores and Hausdorff distances for each patient.

Method	Dice score	Hausdorff distance (mm)
GC	0.8895 (0.0464)	4.8672 (1.8409)
Restricted MI	0.8762 (0.0387)	5.4005 (0.8385)
MI	0.4280 (0.2078)	16.4683 (7.7368)

Table 1. Scores obtained from the three methods.

4. CONCLUSION & DISCUSSION

In this paper, a new framework to propagate the manual delineation of the prostate from MRI onto the CT image was developed. Firstly, an SVM classifier allowed to partially extract the prostate contours in CT image. Then, a new similarity measure based on the contour matching was used to propagate the delineation. Evaluations, achieved on the proposed method and the MI-based registration with two differents ROIs, shown that our method outperformes mutual information when using the same ROI, and slightly improves MI when using a restricted ROI, according to the Dice coefficient and the Hausdorff distance. As a conclusion, it appears that the proposed method provides better results than the traditionally used mutual information when registering prostate MR and CT images, and

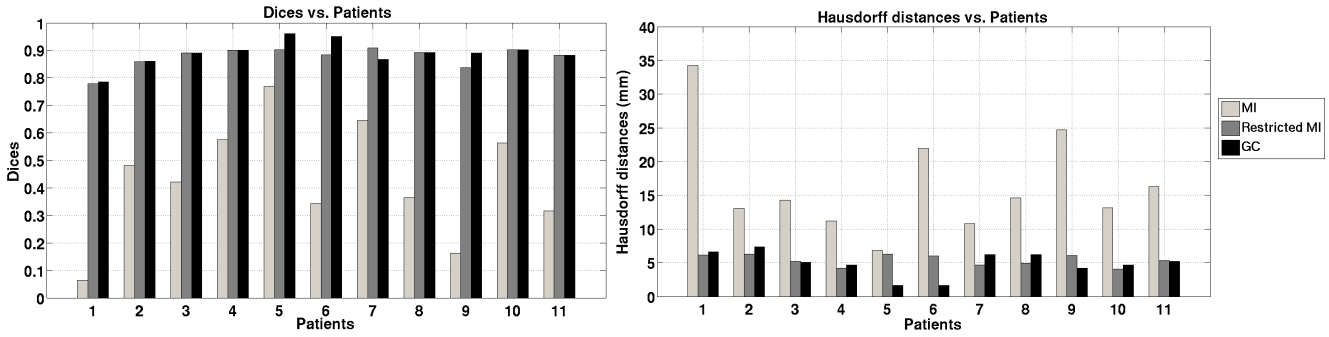

(a) Dice scores obtained for the three methods.

(b) Hausdorff distances (mm) obtained for the three methods.

Fig. 4. Dice scores and Hausdorff distances obtained for the three methods.

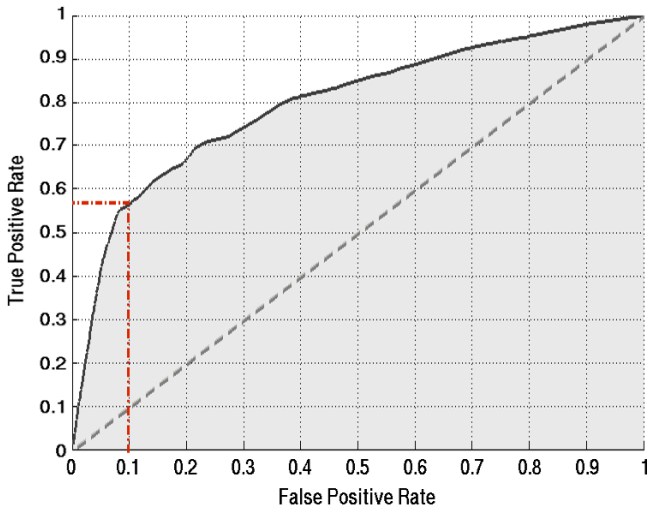

Fig. 3. True positive rate versus false positive rate (ROC curve). Red axis specify the sensitivity for the selected FP rate.

is free from tuning. This study enable the clinical use of the proposed method to align the prostate delineation from MRI onto the CT during the treatment planning, as an accurate fully automatic process, in stead of using a manual expert-dependent registration. Future work will include the use of the gold markers for the validation of the proposed method.

5. REFERENCES

[1] C.Fiorino, *et al.*, "Intra- and inter-observer variability in contouring prostate and seminal vesicles: implications for conformal treatment planning," in *Rad. Onc.*, vol. 47, no. 3, pp. 285 – 292, 1998.

[2] B.Al-Qaisieh, *et al.*, "Impact of prostate volume evaluation by different observers on CT-based post-implant dosimetry," *Rad. Onc.*, vol. 62, no. 3, pp. 267 – 273, 2002.

[3] C.C. Parker, *et al.*, "Magnetic resonance imaging in the radiation treatment planning of localized prostate cancer using intra-prostatic fiducial markers for computed tomography co-registration," *Rad. Onc.*, vol. 66, no. 2, pp. 217 – 224, 2003.

[4] J.Van Dalen, *et al.*, "Semi-automatic image registration of MRI to CT data of the prostate using gold markers as fiducials," vol. 2717 of *MICCAI*, pp. 311–320, 2003.

[5] P. W. McLaughlin, *et al.*, "The use of mutual information in registration of CT and MRI datasets post permanent implant," *Brachytherapy*, vol. 3, no. 2, pp. 61 – 70, 2004.

[6] G. J.Van Der Wielen, *et al.*, "Deformation of prostate and seminal vesicles relative to intraprostatic fiducial markers," *Int. Journ. of Rad. Onc.*, vol. 72, no. 5, pp. 1604 – 1611, 2008.

[7] J.Cai, *et al.*, "CT and PET lung image registration and fusion in radiotherapy treatment planning using the chamfer-matching method," *Int. Journ. of Rad. Onc.*, vol. 43, no. 4, pp. 883 – 891, 1999.

[8] M. Van Herk, "Chapter 35 - image registration using chamfer matching," in *Handbook of Medical Image Processing and Analysis*, pp. 591 – 603, 2009.

[9] L.Shang, *et al.*, "Rigid medical image registration using PCA neural network," *Neurocomputing*, vol. 69, no. 13–15, pp. 1717 – 1722, 2006.

[10] P.Wen, "Medical image registration based-on points, contour and curves," *ICBEI*, vol. 2, pp. 132–136, 2008.

[11] A. Wong, *et al.* "Efficient least squares fusion of MRI and CT images using a phase congruency model," *Pattern Recognition Letters*, vol. 29, no. 3, pp. 173 – 180, 2008.

[12] Y. Gao, *et al.*, "Prostate segmentation by sparse representation based classification," in *MICCAI*, 2012.

[13] R. Lienhart, *et al.*, "An extended set of haar-like features for rapid object detection," in *ICIP*, 2002, vol. 1, pp.900 – 903.

[14] O. Acosta, *et al.* "Evaluation of multi-atlas-based segmentation of CT scans in prostate cancer radiotherapy," in *IEEE ISBI*, 2011, pp. 1966 –1969.

[15] J.A. Dowling, *et al.*, "An atlas-based electron density mapping method for magnetic resonance imaging (MRI)-alone treatment planning and adaptive MRI-based prostate radiation therapy," *Int. Journ. of Rad. Onc.*, vol. 83, no. 1, pp. e5 – e11, 2012.

[16] F. Commandeur, *et al.*, "A vtk algorithm for the computation of the hausdorff distance," p. http://hdl.handle.net/10380/3322, 09 2011.